Fermilab

Doc Number: Beams-doc-2803
Version: 1.0
Type: Note

Measurement of Booster Beam Halo using the C836A and C838A Collimators in the MI8 Beamline

Bruce C. Brown
Main Injector Department
*Fermi National Accelerator Laboratory**
P.O. Box 500
Batavia, Illinois 60510

11 June 2007

*Operated by the Fermi Research Alliance under contract with the U.S. Department of Energy

Measurement of Booster Beam Halo using the C836A and C838A Collimators in the MI8 Beamline

Abstract

During high intensity operation for NuMI, the MI8 Collimators have been used to measure the halo in the horizontal and vertical planes. The collimators are positioned to scrape the beam halo. Losses were recorded using LM8C1 through LM8C4 whose response is shown to be approximately linear with lost beam intensity. Measurements are reported using the MI836A collimator and 90^{o} phase advance downstream at C838A. The sensitivity was calibrated using the change in transmission from toroids I:TOR806 to I:TOR852. The integrated loss is found to be exponential from above 1% to nearly 0.01% or below. The sensitivity of the halo measurement is limited by a measured loss which is independent of collimator positioning.

Introduction

Since commissioning the MI8 Collimators in January 2007 (see Beams-doc-2618), the MI8 Beam has been collimated at 836 and 838. This study has re-measured the sensitivity of the loss monitor system, shown that it responds linearly to losses originating from a given collimator jaw (top, bottom, left, right), but responds somewhat differently to the same loss created on another jaw, and has documented the halo shapes using each of the four jaws of the C836A and C838A collimators. Other effects concerning losses both locally and downstream are noted.

Measurement Setup

Attempts to make this measurement with 'knob-plots' with the Fast Time Plot facility were found to be unsatisfactory. Using the I88 histogram facility, the values of 4 parameters
were recorded. In later measurements, two copies of I88 were employed. For example, C836AV measurements used the following histograms and the graphs were stored in the E-Log:

C836AV, TOR852/TOR806, LM8C1, LM8C2
TOR806, VP836, VP837, VP838

Data was recorded by I88 on T:UFEVT (User Friendly Event Timer) which was set to sample on $23 events after data from one of the NuMI beam pulses was available. When the system was ready to record data, the collimator locations were documented in the E-Log from I63<34> and the collimators were moved to non-scraping locations (the faster-moving horizontal collimators were moved to position 0 while the slower-moving vertical collimators were moved to positions hundreds of mils from the scraping location.

When preparations for the measurement were complete, a collimator for study was moved to a desired location and the histograms in the two I88 instances were started. Twenty or more pulses were recorded. Copies of the graphs were stored in the E-Log and the collimator position was changed. Typically the sequence was to move from the initial nominal location where a fraction of 1% was scraped, toward a high scrape (few percent), then stepping back through the 1% region and across to center the collimator. Periodically, histograms of the Texas Multiwires, especially the 836 Horizontal and 836 Vertical were also recorded in the E-Log. When data was complete for one jaw, the collimator move was continued beyond 0 to scrape with the other jaw.

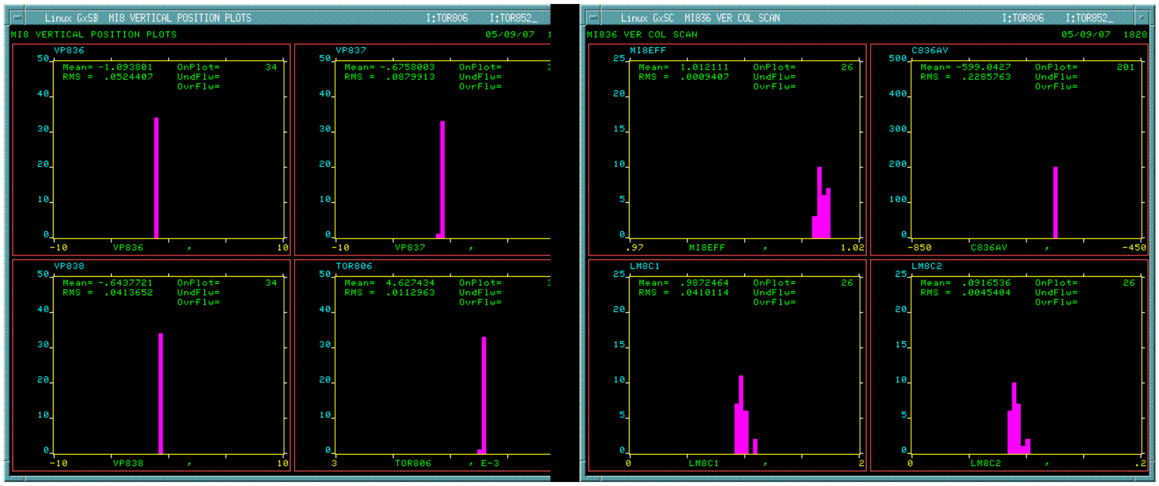

Figure 1. Typical I88 Histograms for MI8 Collimator Study

Loss Monitor Calibration Data

The toroids calibrations differ by up to several percent. Additionally, the beam transmission varies with Booster beam quality and the beamline tune-up. However, the efficiency remains quite steady for hours at a time when external programmatic changes do not cause intensity or other variations. This permits us to calibrate the ionization loss monitors against transmission. Loss monitor LM8C1 is located adjacent to the 836 Marble Mask, LM8C2 is against the wall above and just downstream of the Marble Mask, LM8C3 and LM8C4 mimic the LM8C1 and LM8C2 locations in the 838 half-cell.

Figure 2. Loss Monitor LM8C1 is shown adjacent to the Marble Mask. Loss Monitor LM8C2 is visible at the top of the picture, hanging on the wall.

Loss Monitor	LM8C1	LM8C2	LM8C3	LM8C4
Units	Protons/(R/s)	Protons/(R/s)	Protons/(R/s)	Protons/(R/s)
From Hor Positive	1.18E+10		7.03E+09	
From Hor Negative	1.30E+10		1.07E+10	
From Vert Positive	1.5178E+10	1.0685E+11	1.1035E+10	9.8180E+10
From Vert Negative	9.5584E+09	9.7697E+10	9.19E+09	7.94E+10

Table 1. Sensitivity of LM8C1 and LM8C2 to losses due to C836A. Sensitivity of LM8C3 and LM8C4 to losses due to C838A. See fits results in the following figures.

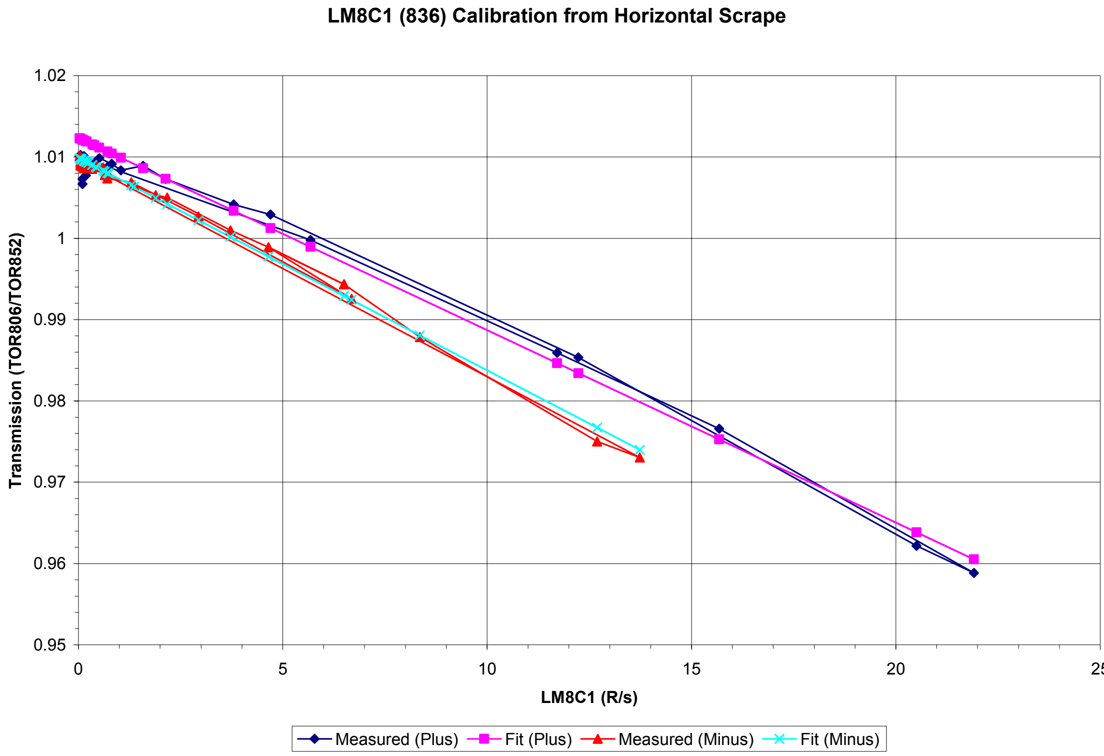

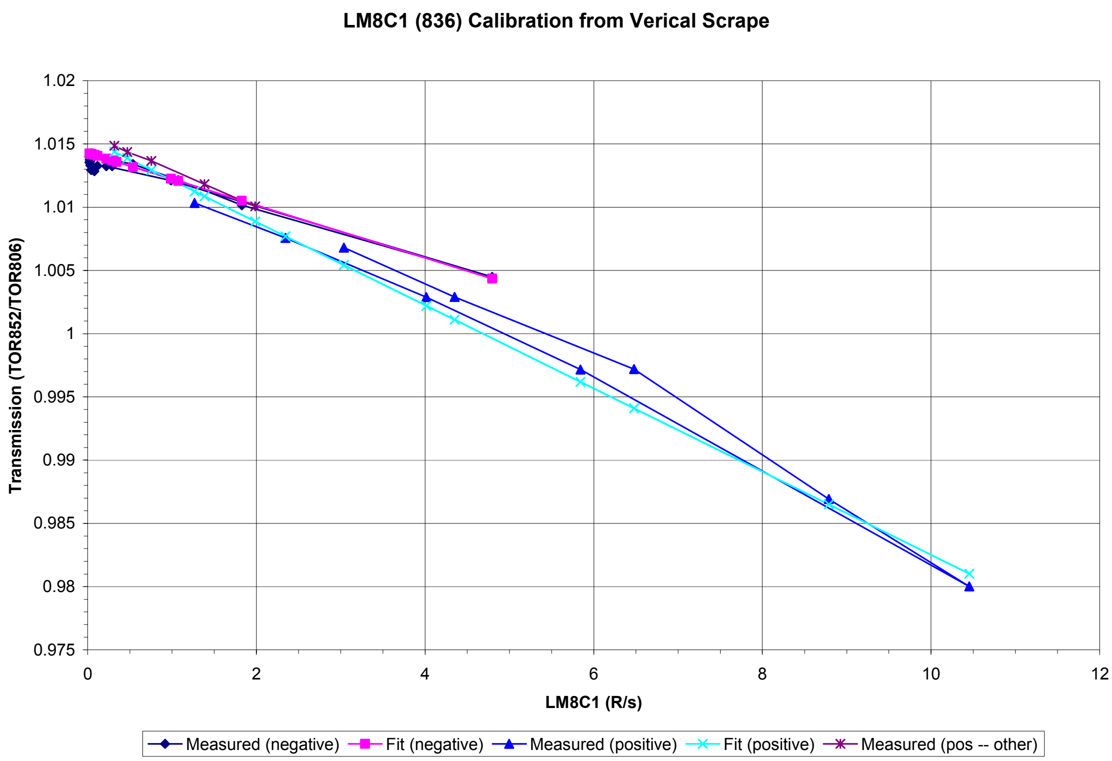

Figure 3. Calibration of LM8C1 vs. Transmission using horizontal scans (top) and vertical scans (bottom).

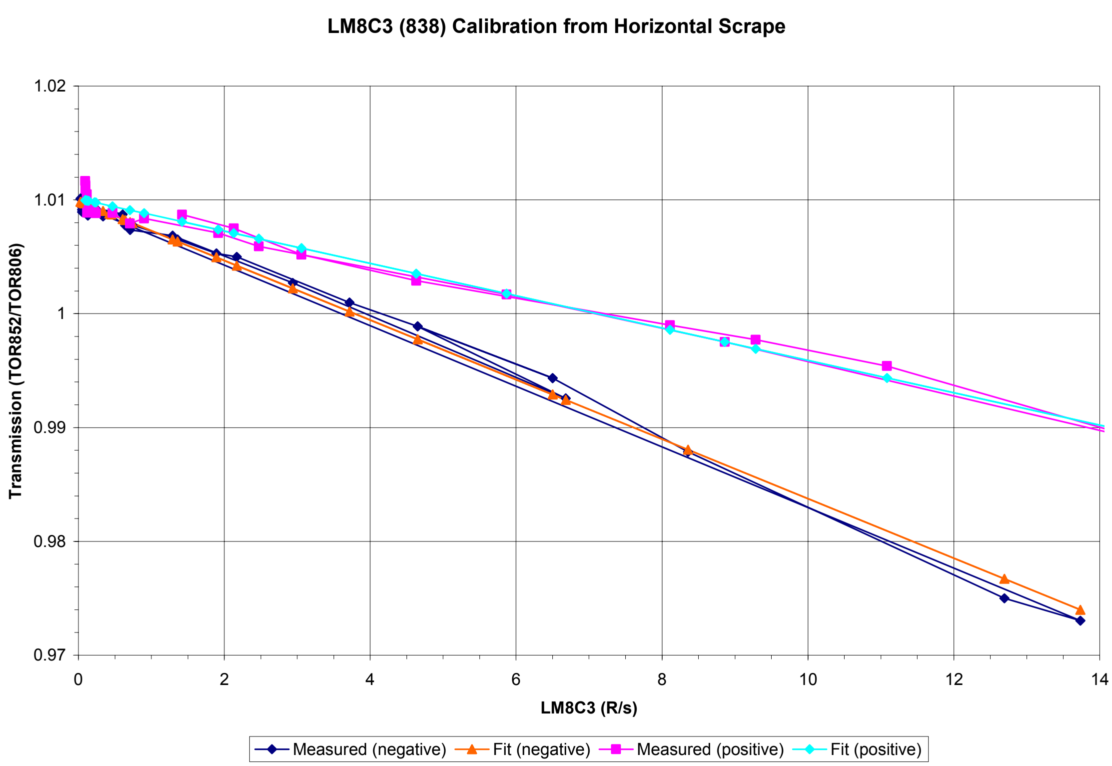

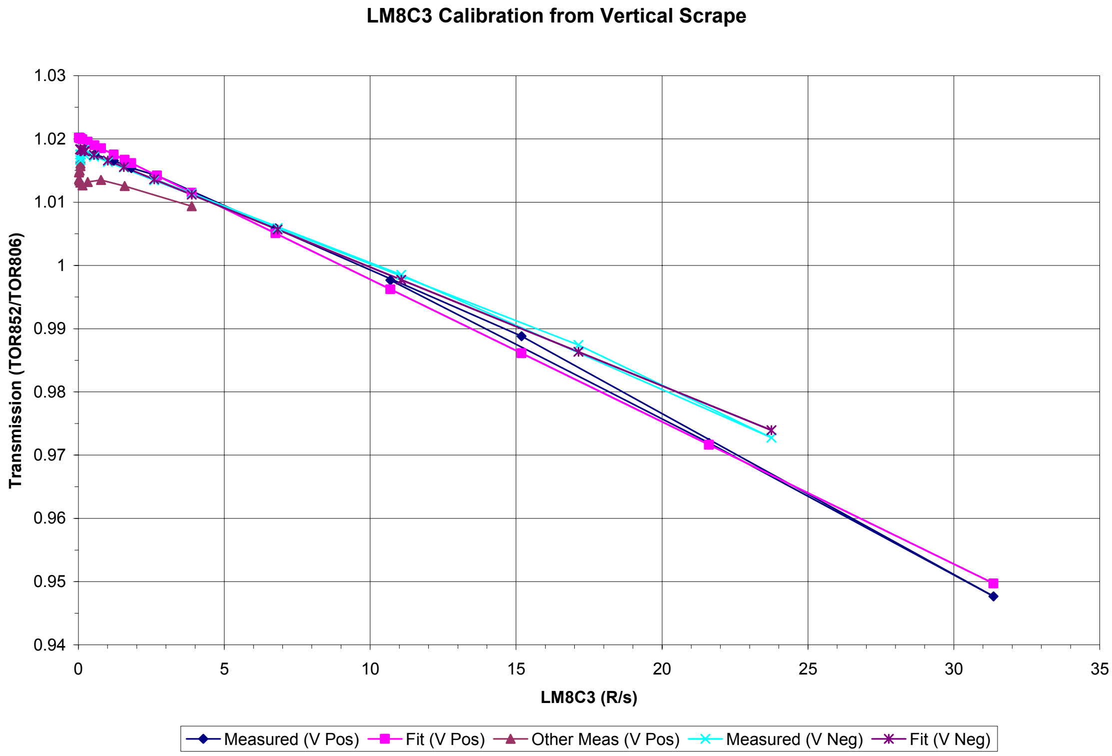

Figure 4. Calibration of LM8C3 vs. Transmission using horizontal scans (top) and vertical scans (bottom).

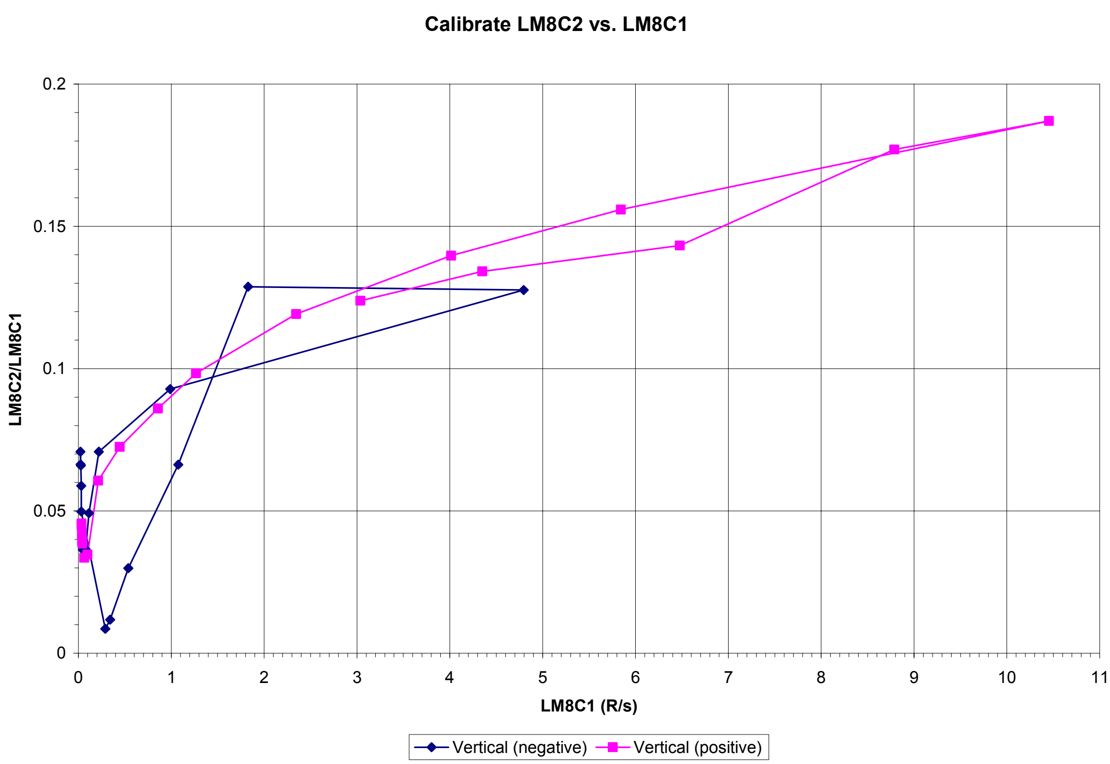

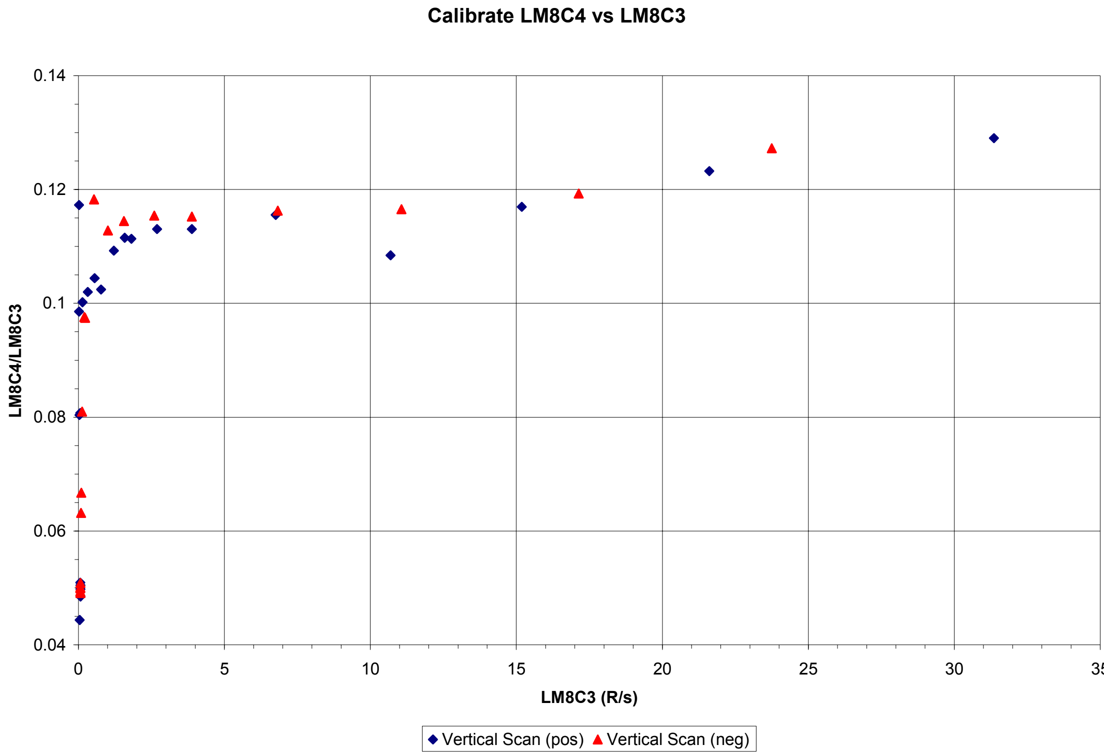

Figure 5. Calibration of LM8C2 vs. LM8C1 (top) and LM8C4 vs. LM8C3 (bottom)

Beam Profile Data and Results

In order to study the beam profile, we first convert the loss monitor readings to the lost beam intensity. Using a linear fit to Transmission (TOR852/TOR806) vs. Loss (LM8C1 or LM8C3) as shown in Figure 3 and Figure 4, we find a slope and intercept. The slope (loss fraction/(R/s) is converted to a sensitivity (Lost Protons/(R/s)) by multiplying by the average Booster beam pulse intensity (<TOR806>). These calibration values are shown in Table 1. Most of the data is taken with constant Booster intensity (about 5E12 p/pulse) but we plot the beam fraction vs. collimator position to further minimize the effects of intensity variation. Figures 6 – 9 show the beam loss profile for each axis of motion of C836A and C838A. We plot to lost protons (integrated), not the local intensity since that is what is directly measured. Note that the motion is labeled by the collimator position so the beam edge which is scraped is opposite.

We see in Figure 5 that the response of LM8C4 is mostly proportional to the LM8C3 measurement of loss. There is a clear tendency for higher losses to produce more than linearly higher response in LM8C4 but the effect is modest (about 10%). Using the average ratio LM8C4/LM8C3, a calibration for LM8C4 is shown in Table 1. The response of LM8C2 is much more loosely correlated with the loss recorded by LM8C1. The average of some points with moderate lost beam is used to provide a nominal calibration for LM8C2. One should assume that this determination has large errors.

Using this calibration (for each end of each axis) we convert our measurement of loss monitor reading vs. collimator position to produce plots of integrated loss vs. collimator position. Figures 6 – 9 show these results. The data is clearly quite exponential except for the portion which is independent of collimator position. We find that almost all the data is well represented by an exponential fall plus a constant background. The background is due to the loss observed by the loss monitor which is independent of the collimator position (probably due to upstream sources). It is typically a signal corresponding to a local loss of about 10-4 of the beam. The constant term is subtracted off and the Excel fit function, LOGEST, is used to a capture the exponential shape.

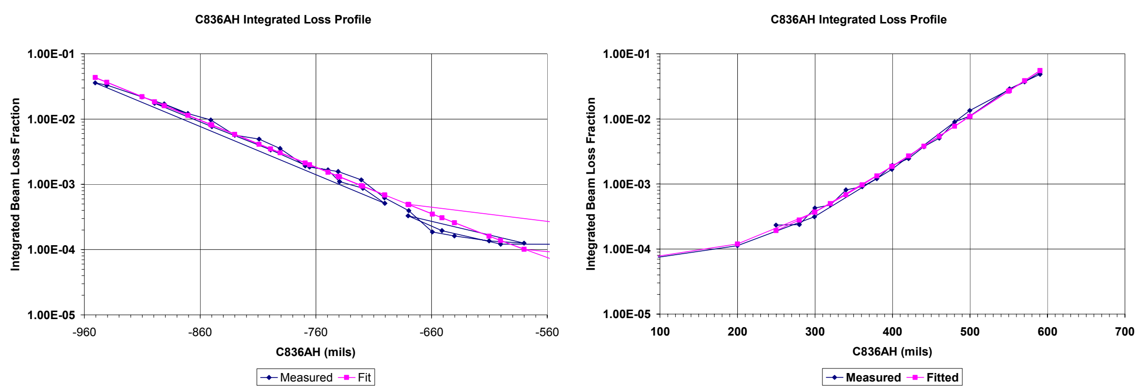

Figure 6. Horizontal Lost Beam Profiles at C836A

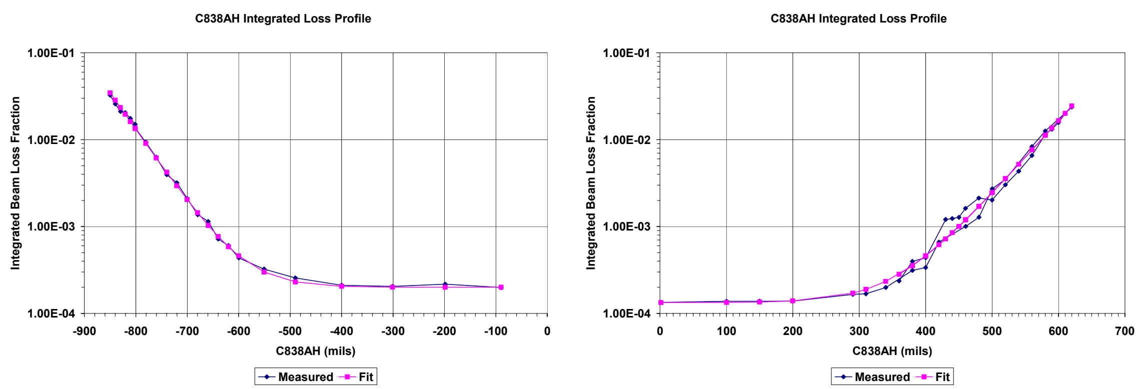

Figure 7. Horizontal Lost Beam Profiles at C838A

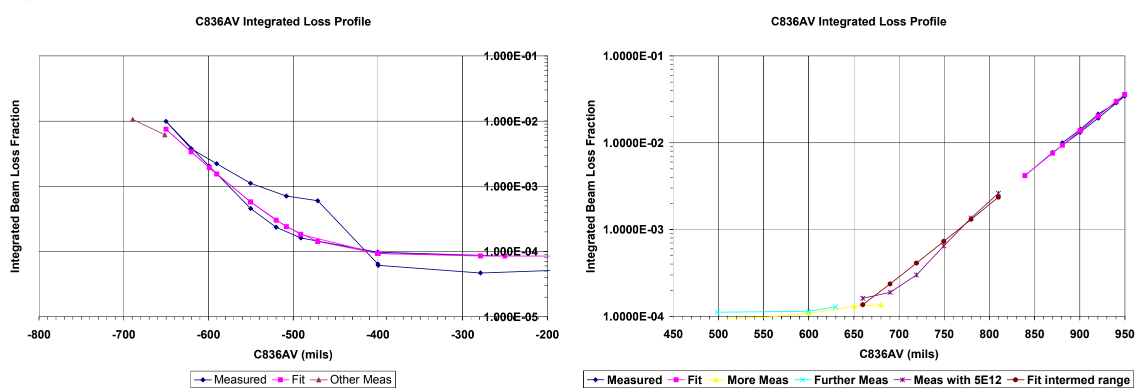

Figure 8. Vertical Lost Beam Profiles at C836A

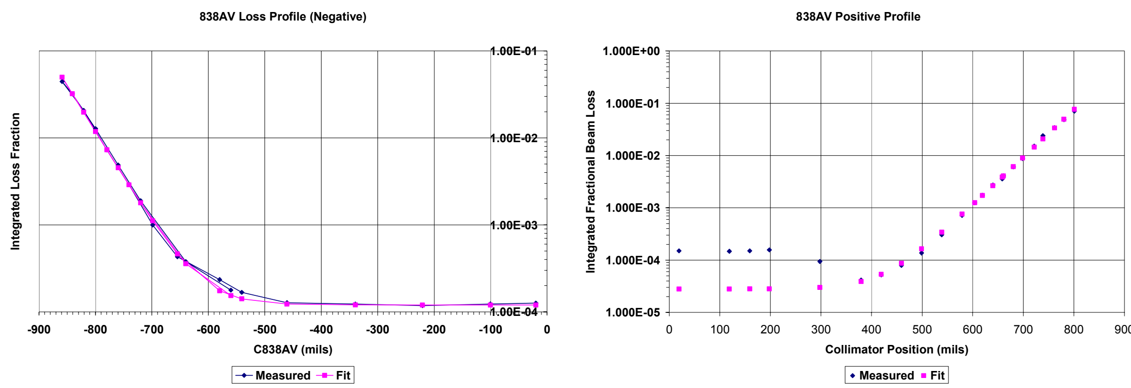

Figure 9. Vertical Lost Beam Profiles at C838A

We stopped the scraping without scraping the core of the beam. The Gaussian profile measured (and fit) by the multi-wire systems appears to provide a good representation of the beam core. We can use the measured sigma at 836 to predict widths at C836A and C838A based on measured beta values. The match was fairly satisfactory but it was decided that a comparison of the shape would be more effective if the mean and sigma was adjusted. In practice, the assumed beta and center were adjusted to visually match the Gaussian to the measured halo distributions. The above data along with the Gaussians were re-plotted in Figures 10 – 13 to show integrated loss vs. beam edge

edge = ±1000 +collimator position.

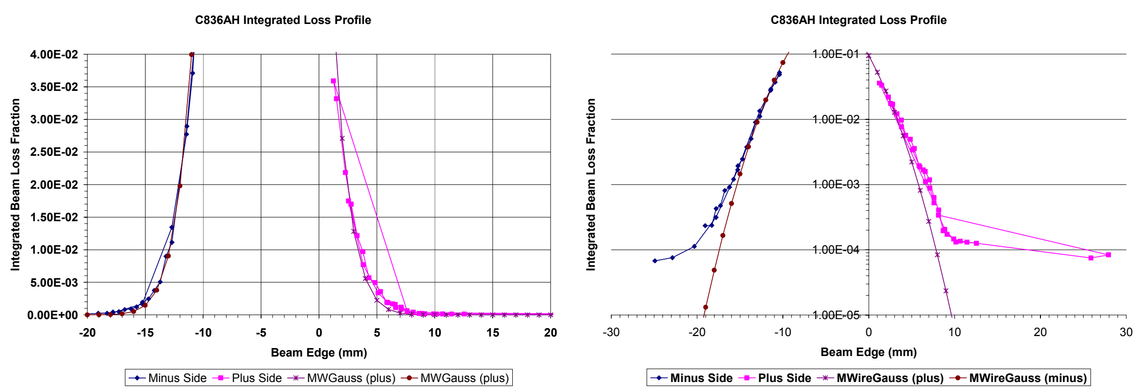

Figure 10. Integrated Beam Loss Profile at C836AH.

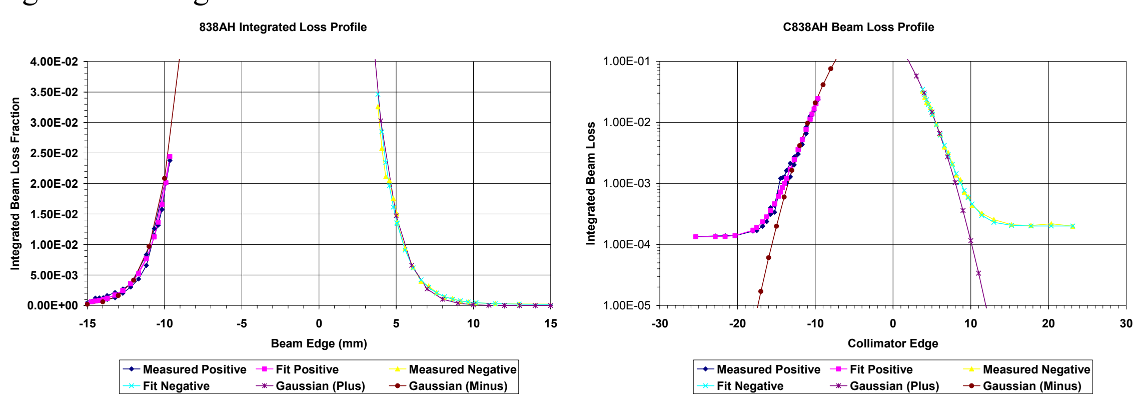

Figure 11. Integrated Beam Loss Profile at C838AH.

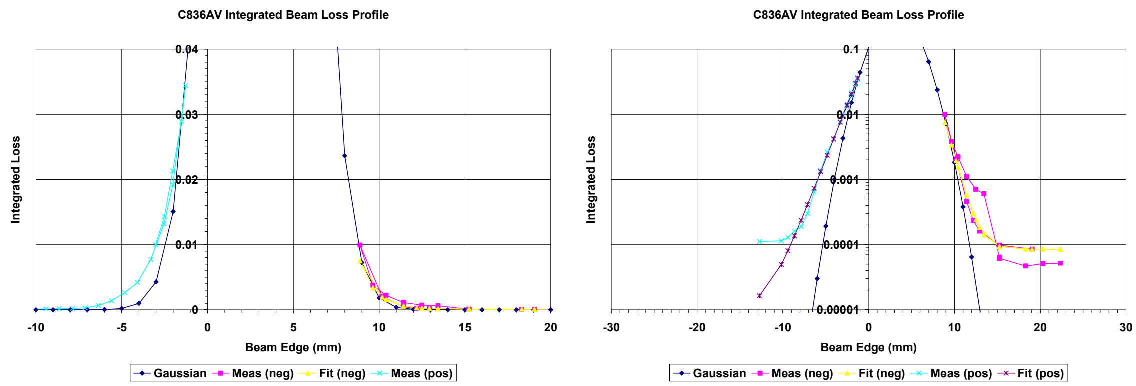

Figure 12. Integrated Beam Loss Profile at C836AV.

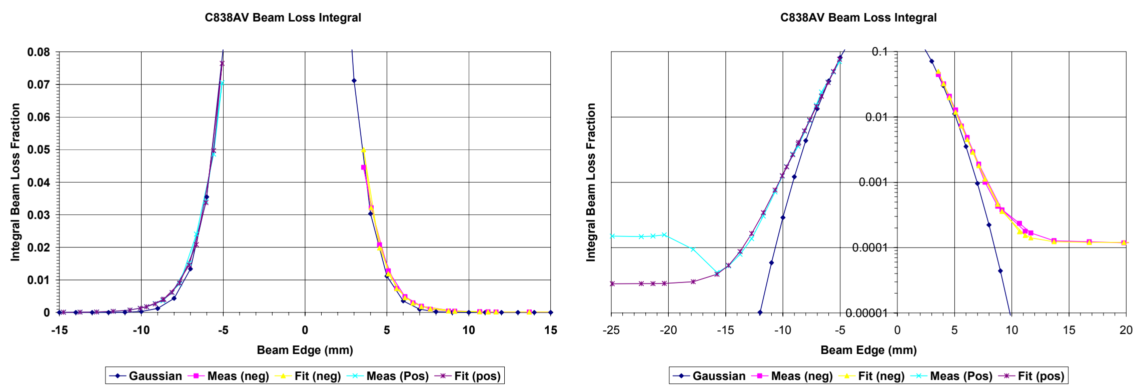

Figure 13. Integrated Beam Loss at C838AV.

It is of direct interest for operations to determine whether the halo is symmetric. Since one edge will be scraped by the A collimator and the opposite edge by the B collimator, if an asymmetry is demonstrated, then one may wish to optimize this choice. To examine the symmetry, the data in Figures 6 – 9 has been re-plotted with the collimator negative reading reversed and an offset added. The offset was adjusted to visually match the integrated loss at high loss levels. These results are shown in Figures 14 and15.

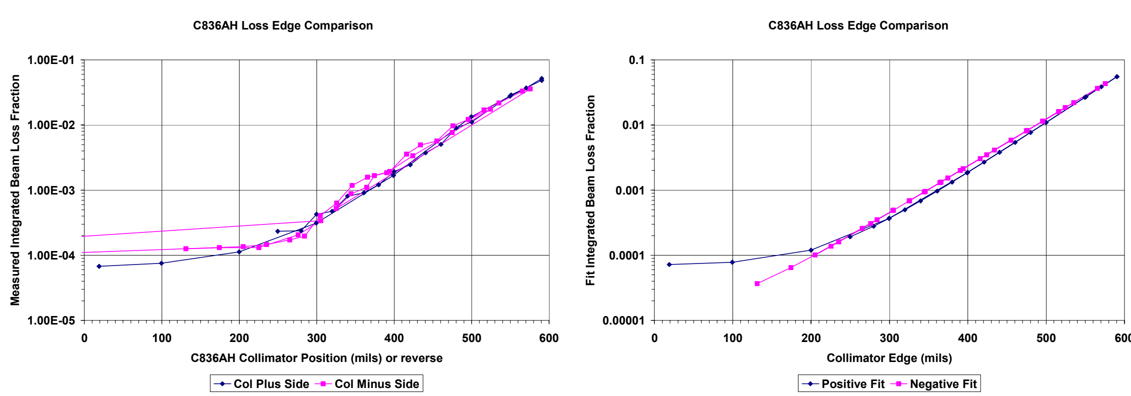

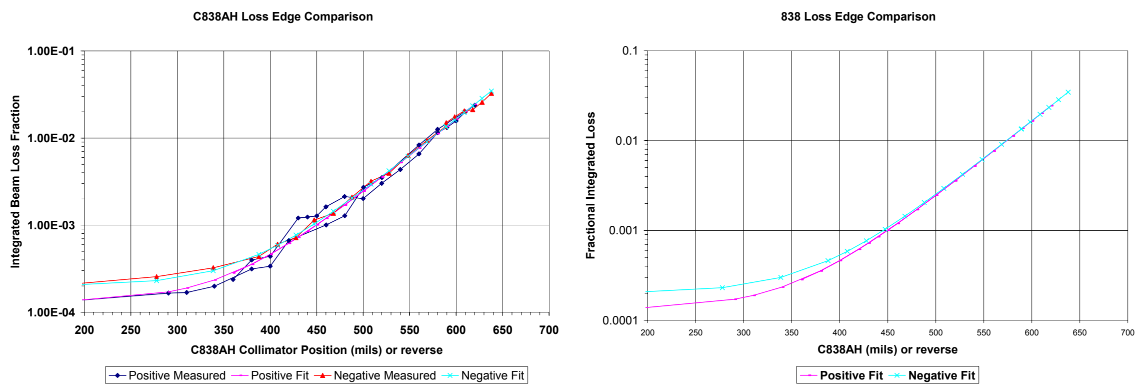

Figure 14. Comparison of beam edges. Above for C836AH, Below for C838AH, Left for measurements, right for exponential fits to measurements.

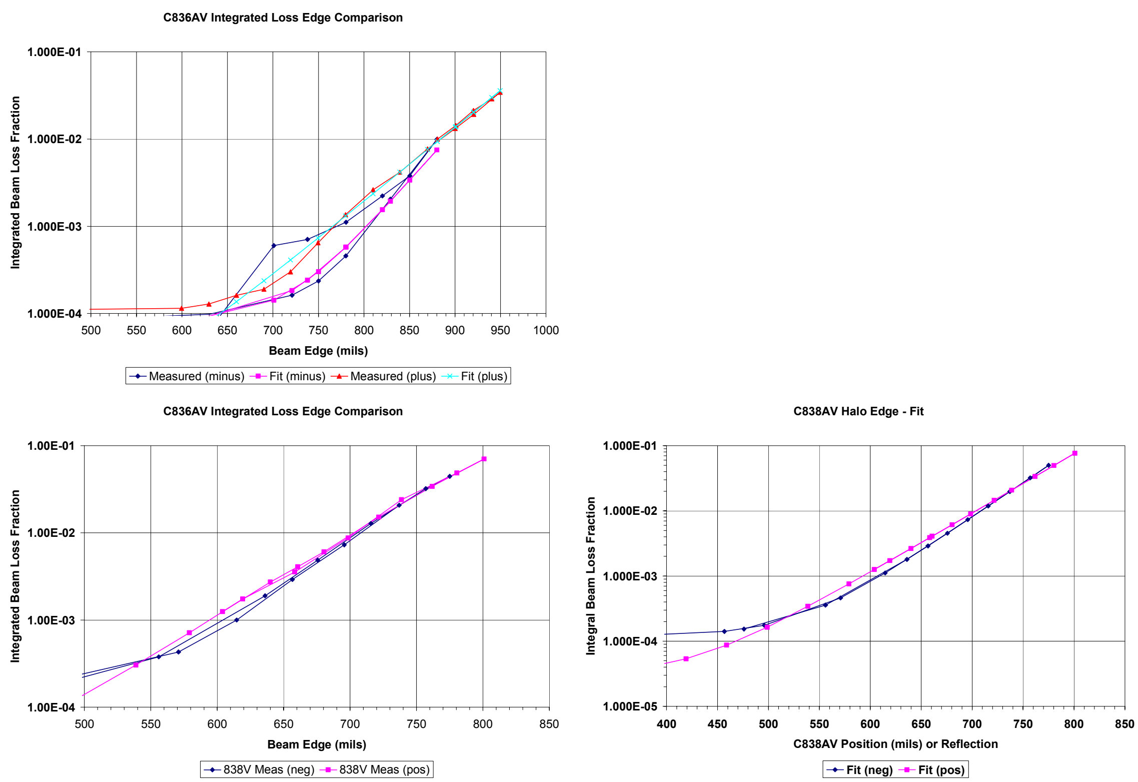

Figure 15. Comparison of beam edges. Above measured and fit for C836AV. Below left C838AV measured. Below right C838AV fit.

Using the LOGEST fits shown in the above figures, one can get a representation of the halo which is more physically obvious by converting from the power-law representation to an exponential representation. We choose to show the results for a normalization at the 1% integrated loss point as follows:

LOGEST: $y = b * m^x$

Table II: $y = 0.01 \exp((x - x_0) / a)$

a = -1 / (ln m) ; x_0 = -ln(100 *b) / (ln m)

The collimator position is reported in the same coordinate system orientation as is the beam profiles so positive is above or to the right. The above values of x_0 give the collimator position at which the collimator scrapes 1% of the beam. We will use X_0 to define the beam coordinate for which 1% of the beam lies at a larger distance from the beam center. Thus for the positive edge of the beam, we use measurements with the negative collimator setting and the 1% edge of the beam is given by X_0 = 25.4 + x_0 (assuming x_0 has been converted to mm). For the negative edge of the beam, the X_0 = -25.4 + x_0. Table II will show the fit quantities converted to exponential format.

Table II: Fitted Results for Exponential (10-2 exp(-(x-x0)/a)

	a		x_0		X-0		Width (98%)	Center
	mm	mm	mm	Mm	mm	mm	mm	Mm
	Negative	Positive	Negative	Positive				
836AH	1.527737	-1.41537	-21.9094	12.58068	3.490604	-12.8193	16.30993	-4.66436
838AH	1.30119	-1.29762	-19.9798	14.5959	5.420246	-10.8041	16.22435	-2.69193
836AV	0.93456	-1.30073	-16.7922	22.45753	8.607842	-2.94247	11.55031	2.832687
838AV	1.041336	-1.21198	-20.1474	17.87796	5.252579	-7.52204	12.77462	-1.13473

Table III: Lattice Beta Values

	MJY Oct06		Gaussian	
	Beta_x	Beta_y	Beta_x	Beta_y
836	41.08	8.65		
C836A	28	16.6	28	14
C836B	25.5	18.7		
838	48.7	13.6		
C838A	34.1	22.9	29	17
C838B	31.1	25.3		

The MI8 lattice has been measured and adjusted several times by Ming-Jen Yang. Table III Columns 2 and 3 show results the current lattice tune which was measured in October 2006. Columns 4 and 5 show the beta values which were employed to achieve the results shown in Figures 10 – 13. We note that the agreement is good for C836AH but the other three profiles are fit with an apparently narrower Gaussian profile. The beam center is found from these scans is a few mm different than that inferred from the beam position monitors which are in the same region. We note that VP836 is immediately upstream of C836A so little interpolation is required. These discrepancies may bear further examination.

Further Discussion

A few items noted during these measurements are worth calling to our attention. The naïve interpretation of the loss monitor readings in the regions beyond the exponential fall would be that the radiation is from upstream and not related to the losses on that collimator. We note, however, that some of the scans show some distinctive features:

- The loss pattern on the beam right (collimator negative) shows a flattening at about 1.3E-4 of the beam but later falls to 0.8E-4.

- The differences in loss plotted on the left and right side of C838AH is due to the different calibration applied. The measured loss monitor readings were more similar.

- The scan on C836AV negative collimator side was made more challenging by numerous changes in Booster operation, both timeline changes for NuMI only vs. Mixed Mode and many changes in the intensity (number of Booster turns. The two very different levels of loss on the positive edge of the beam between 10 mm and 15 mm were observed. Further study would be required to determine if the higher level is repeatable or if beam conditions which caused it can be controlled to avoid the higher loss.

- On the negative side of the beam at C838AV (positive collimator position), the beam loss fell to a very low level of 4E-5 for C838AV = 380 mils but scanning further to the middle showed higher losses of around 1.4E-4. Whether the very low reading is due to some masking of LM8C3 or some other effect has not been determined. It was repeatable for one or two additional measurements.

It was noted that the peak scraping resulted in higher losses both in the MI8 line to the Main Injector and in the MiniBooNE line. Further investigation of this may be warranted.

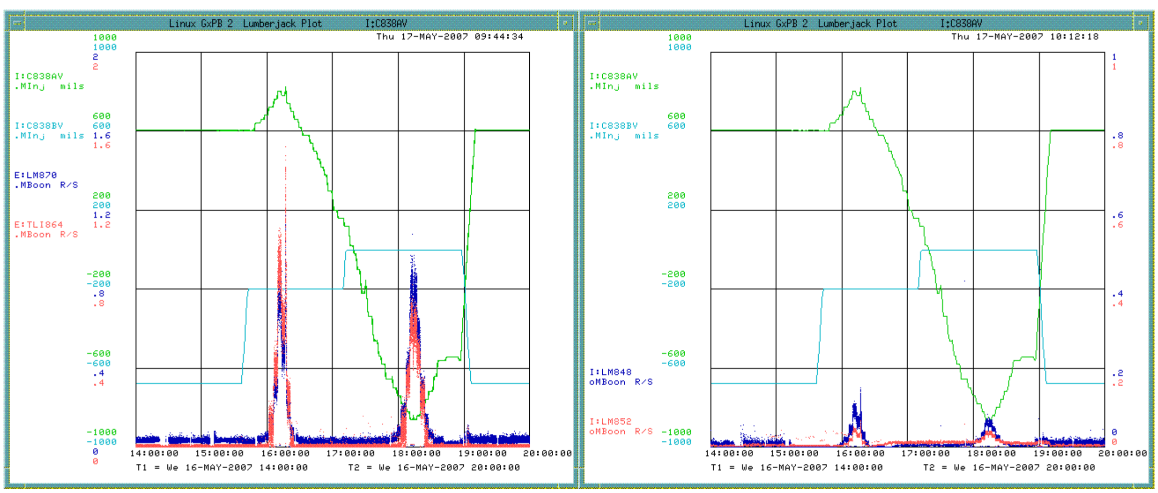

Figure 16. Losses reported by D44 Datalogger during scan of C838AV. Left is losses at LM870 and TLI864. Right is losses at LM848 and LM853.

These results were obtained on April 9, May 9 and May 16, 2007. The measurements are in the Main Injector E-Log. The data analysis was carried out with EXCEL and the spreadsheet (MI8_Col_Scrape_Spring_2007.xls) is stored as a part of this document (Beams-doc-2803).

Conclusions

The loss monitors have been calibrated by comparing the loss monitor response to the number of protons lost on the 'A' collimators. The LM8C1 and LM8C3 show a linear response to the number of lost protons with average response of 1.24E+10 protons / (R/s) for LM8C1 and 9.49E+09 protons / (R/s) for LM8C3.

We have demonstrated that beyond the Gaussian central portion of the MI8 Beam, we have measured halo (beam tails) which are substantially above the Gaussian projection. These tails are well described by exponential distributions. Note that we have fit an exponential to the integrated loss vs. position, but this would also imply an exponential distribution of the beam intensity profile. In Table II, we show that the beam tails in the horizontal plane are fairly symmetric with the 'a' parameter being 6% larger on the beam positive side (collimator negative side) at C836AH and less than 0.3% larger for the C838AH measurement. However, the situation in the vertical plane demonstrates asymmetric halos with the 'a' parameter being 40% larger (halo falls off more quickly) on the downward (beam negative or collimator positive) side at C836AV and 16% larger at C838AV.

Acknowledgments

The assistance of Denton Morris, Dave Capista, Phil Adamson, Dave Johnson and especially Ming-Jen Yang are gratefully acknowledged.